Hypersatellite and satellite transitions in xenon atoms

Ilakovac, Ksenofont; Vesković, M.; Horvat, V.; Kaić, S.

Hypersatellite and satellite transitions in xenon atoms

K. Ilakovac
Department of Physics, Faculty of Science and Mathematics, University of Zagreb, P.O. Box 1016, 41001 Zagreb, Yugoslavia and R. Bošković Institute, P.O. Box 1016, 41001 Zagreb, Yugoslavia

M. Vesković
Institute of Physics, University of Novi Sad, Ul. Dr. I. Duričića 4, 21000 Novi Sad, Yugoslavia

V. Horvat
Faculty of Science and Mathematics, University of Zagreb, P.O. Box 162, 41001 Zagreb, Yugoslavia

S. Kaučić
R. Bošković Institute, P.O. Box 1016, 41001 Zagreb, Yugoslavia
(Received 31 July 1989; revised manuscript received 17 October 1989)

Decay of double-K-shell-vacancy states in xenon atoms, created in the decay of ^{131}Cs, was investigated. The measurements were performed with a pair of germanium detectors, a fast-slow coincidence system, and a three-parameter pulse-height analyzer. In the analysis of the two-dimensional E_1-E_2 spectrum, improved least-squares routines were applied. The following results were derived: the probability of creation of a double K-shell vacancy per ^{131}Cs decay, $P_{KK}=(1.48\pm0.35)\times10^{-5}$; the hypersatellite energy shifts $\Delta^h(K\alpha)=(653\pm20)$ eV, $\Delta^h(K\beta_1)=(834\pm39)$ eV, and $\Delta^h(K\beta_2)=(903\pm81)$ eV; the average values of the satellite energy shifts due to the presence of an L_3- or L_2-shell spectator vacancy $\Delta^s(K\alpha L^{-1})=(80\pm15)$ eV, $\Delta^s(K\beta_1L^{-1})=(169\pm34)$ eV, and $\Delta^s(K\beta_2L^{-1})=(261\pm81)$ eV; the intensity ratios of the hypersatellite transitions, $I(K\alpha_2^h)/I(K\alpha_1^h)=0.94\pm0.18$, $I(K\beta_1^h)/I(K\alpha_1^h)=0.36\pm0.06$, and $I(K\beta_2^h)/I(K\alpha_1^h)=0.09\pm0.04$; the intensity ratios of the satellite transitions $I(K\alpha_2L^{-1})/I(K\alpha_1L^{-1})=0.44\pm0.10$ and 0.44 ± 0.09 for an L_3 and L_2 spectator vacancy, respectively; and the intensity ratios of some other satellite transitions.

INTRODUCTION

Removal of both electrons from the K shell of an atom yields a very highly excited state. The double K-shell vacancy (K^{-2}) state decays rapidly by a succession of transitions. Many of the intermediate states are also highly excited atomic states with two or more vacancies in the shells. The first and the second transition of electrons from higher shells, which fill the two K-shell vacancies, are considered to occur predominantly by the emission of a hypersatellite and of a satellite K x ray. The first transition occurs in the presence of a "spectator" vacancy in the K shell. This vacancy causes considerable changes of states of electrons when compared to the states observed in atoms with an initial single K-shell vacancy (which gives rise to the emission of the diagram lines). The changes are observed as shifts in energy of the emission spectra (the hypersatellite energy shifts) and as modified intensity ratios of the K x-ray lines (the hypersatellite intensity ratios). The hypersatellite transition creates a vacancy in the L, M, or N shell. Hence the following satellite transition occurs in the presence of a vacancy in a higher shell. Similar but smaller effects, namely, energy shifts and modified intensity ratios, are observed.

In the original investigation of Briand, Tavernier, and Roset[1] radioactive decay was used to create the K^{-2} states in atoms of gallium, and the coincidence technique was applied to detect the pair of hard K x rays emitted from the atoms and to measure their energy shifts. Since then many experiments were performed in which the hypersatellite (and satellite) transitions were detected either by using semiconductor detectors and the coincidence method[2,3] or by the application of a high-resolution diffraction technique,[4] and the K^{-2} states were created by nuclear decay, or by beams of ions, photons, or electrons.

The theoretical treatment of states and transitions in atoms with two inner-shell vacancies has advanced rather well. Desclaux and co-workers[5] pointed out the importance of relativistic effects, in particular of the Breit interaction. Chen, Crasemann, and Mark[6] made a detailed theoretical study based on the relativistic Dirac-Hartree-Slater (DHS) approximation, including the Breit interaction term, and calculated energy shifts of the states involved in the hypersatellite transitions and the transition rates.

We report an experimental investigation of hypersatellite-satellite cascades in xenon atoms. This is an extension of a previous study by Isozumi, Briançon, and Walen.[3] The K^{-2} states were generated in the electron-capture decay of ^{131}Cs. The coincidence technique was applied and relatively weak sources of ^{131}Cs were used. Due to the very low background a rather clear interpretation of the data was possible.

MEASUREMENTS

Radioactive ^{131}Cs was produced in the nuclear reactor of the Boris Kidrič Institute (near Belgrade), by the irradiation of 3 g of $BaCO_3$, sealed in a quartz ampoule, in a flux of about 3.5×10^{13} neutrons/(cm^2 s) for 135 h. Radiochemical separation and purification of ^{131}Cs was made by the following operations. Cesium was removed from the irradiated sample by triple recrystallization of $BaCl_2$. The purified $BaCl_2$ was introduced into a column filled with the "Bio-Rad" cation exchange resin Dowex 50 WX$^+$, 100–200 mesh. After 14 days, when the maximum radioactivity of ^{131}Cs was expected, elution of cesium with 1N HCl was made. Finally, the solution was introduced into a smaller "Bio-Rad" cation exchange column, followed by elution with 0.5N HCl. The last operation was repeated once. The initial radioactivity of the prepared ^{131}Cs source was about 46 MBq. Its radioactive purity was checked using a Ge(Li) γ-ray spectrometer. Weak contamination by ^{131}Ba, ^{134}Cs, ^{59}Fe, and ^{60}Co was found, their radioactivity being almost eight orders of magnitude less than that of ^{131}Cs.

In the course of the measurements ten weak sources were used. Their initial activities were between 0.9 and 1.2 kBq. Each of the sources was prepared by putting a small droplet of the $^{131}CsCl_2$ solution on a polyethylene sheet, into which a small piece of pure cellulose paper (about 0.4 mm diam) was placed. After drying, the small radioactive piece of paper was placed between two 0.06-mm-thick foils of polyethylene and carefully centered in the hole of the shield. The shield was made of aluminum, its thickness was 2.6 mm, the hole in the shield was of a double-conical form, and the opening (where the source was centered) had a diameter of about 0.7 mm.

The shield with the source was placed between two high-purity germanium planar detectors (supplied by ORTEC, Oak Ridge) of a nominal size 200 mm$^2\times7$ mm thick, in a close 180° geometry. The solid angle subtended from the source of either detector was about 1.6 sr. The short-term energy resolution of the detectors at 5.9 keV was about 230–240 eV, and the long-term resolution at about 30 keV, determined from the complete set of the three-parameter data, was about 375 eV. The time resolution of the system for pairs of photons of energy above 30 keV was about 14 ns.

The fast-slow coincidence system with the three-parameter $128\times512\times512$ pulse-height analyzer recorded the time difference (k_0 channel) and the amplitudes (k_1 and k_2 channel numbers) of pulse pairs arriving from the two detectors within the time resolution of the coincidence unit ($2\tau\approx250$ ns). Prior to the start and after each measurement careful calibration and checks of the apparatus were made. Ten measurements were made, each of 4 to 10 days duration, but the first measurement was rejected because of excessive mains interference. (A faulty apparatus in the vicinity was located and repaired.) The total collection time of the data which were used in the analysis (nine measurements) was 1757 h. The recorded data were analyzed off-line in a UNIVAC 1110 computer, and more recently were reanalyzed in personal computers.

ANALYSIS OF DATA

Two-dimensional spectra are usually analyzed by first making projections of data onto axes. The resulting one-dimensional spectra are then analyzed by standard methods. A detailed analysis of a complex two-dimensional E_1-E_2 spectrum, which was encountered in the measurement described above, would require analysis of about a dozen one-dimensional spectra. Besides, when projecting the data essential information is lost because peaks in the two-dimensional spectrum, which are separated in the direction of projection, merge. For example, if the energy spectra shown in Figs. 2 and 3 were analyzed in this way, it would hardly be possible to determine the parameters of the satellite peaks, even if much better statistics were available.

According to our experience, fitting of a multiparameter surface to a complex two-dimensional spectrum yields much better results. One advantage is that all relevant data are treated simultaneously and all variable parameters are varied concurrently. Therefore the value of each parameter at each step of the search for the minimum χ^2 takes into account the current values of all other parameters. Similarly, when calculating the error of a variable parameter from the curvature matrix, uncertainties of all other parameters are taken into account (actually all errors are calculated simultaneously by inverting the curvature matrix). This is particularly important in the present case because the variable parameters of the fit are considerably interdependent.

For each of the nine measurements projections of the recorded three-parameter data onto the k_0, k_1, and k_2 axes were made and the one-parameter spectra were analyzed. In this way the nine measurements were found to be consistent and all nine records were treated as one set of data.

First analyses were made using the routines described in Ref. 7 (two methods). Data for the $K\alpha$ and $K\beta_1$ hypersatellite, and the $K\alpha$ (L-shell spectator vacancy) satellite energy shifts, for the intensity ratios of hypersatellite and L-shell spectator-vacancy satellite transitions, and for the probability of creation of double-K-shell-vacancy states, P_{KK} (EC) (where EC denotes electron capture), were derived.

Since the energy resolution of the system is comparable to the energy differences of most xenon K x rays detected in the measurement (see Fig. 1), a new routine was written for the analysis of the two-dimensional E_1-E_2 spectrum.

In the following, the standard notation for the diagram K x rays ($K\alpha_1$, $K\alpha_2$, $K\beta_1$, $K\beta_2$) will be extended by writing a superscript h for the hypersatellite transitions, and by adding the designation of the spectator-vacancy shell or subshell for the satellite transitions. For example, $K\alpha_1L_2^{-1}$ will be used to designate a $K\alpha_1$ x ray emitted from an atom with an L_2 spectator vacancy. A real or accidental coincidence event will be denoted by X-Y, where X and Y represent an appropriate pair of notations described above.

All data within a window of the k_1-k_2 field, chosen to accept mainly the real $K\alpha^h$-$K\alpha L^{-1}$ coincidence events,

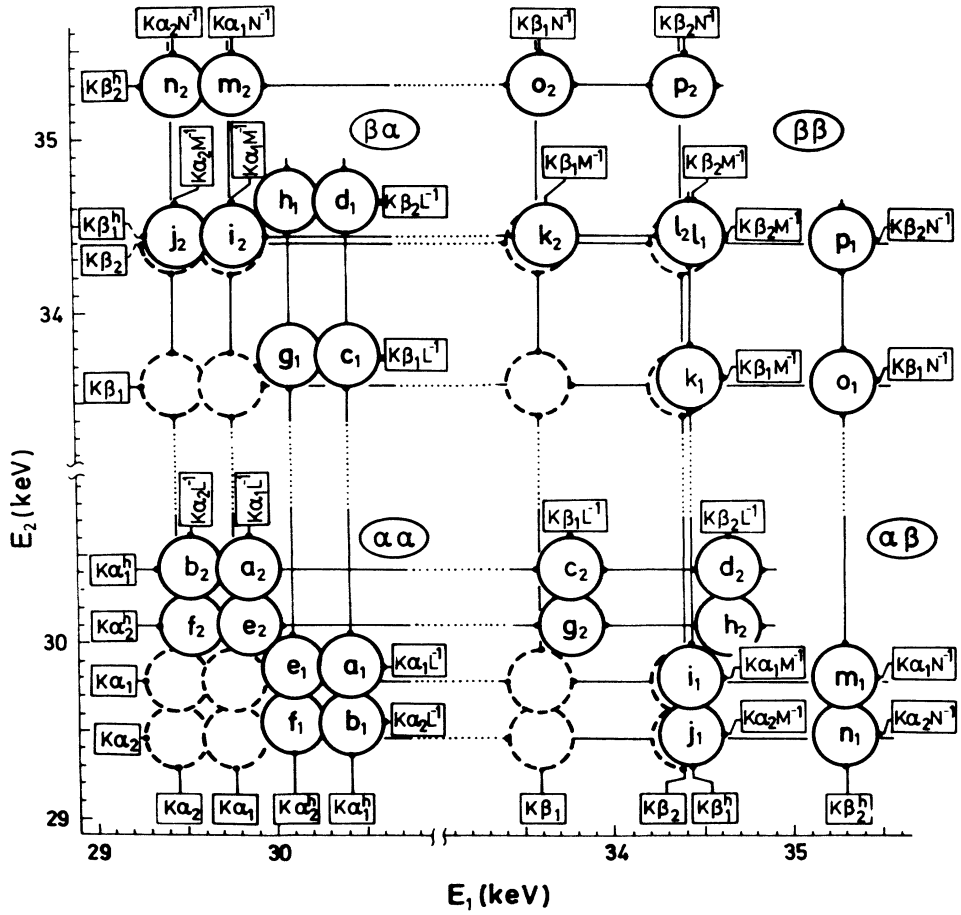

FIG. 1. Schematic representation of the two-dimensional E_1-E_2 spectrum. The dashed circles show 16 peaks due to the accidental coincidences of the diagram K x rays. They are centered on lines indicated by $K\alpha_2$, $K\alpha_1$, $K\beta_1$, and $K\beta_2$. (The energies of the diagram lines are 29.458, 29.779, 33.6, and 34.4 keV.) Solid circles show 16 + 16 peaks due to the real coincidences of the hypersatellite-satellite cascades. The shifts are indicated by the center lines which are marked by the appropriate symbols for the hypersatellite and satellite transitions. The positions of the peaks are drawn to scale and the diameters of the circles indicate the FWHM resolution of the measuring system.

were projected onto the k_0 axis. The time spectrum shows a pronounced peak superimposed upon a (within statistics) constant background. Full width at half maximum (FWHM) of the peak was about five channels, corresponding to a time resolution of about 13 ns. An interval of 12 k_0 channels, which included about 97% of coincidence events, was chosen to make the k_1-k_2 table of "in-coincidence" numbers of events (the two-dimensional E_1-E_2 spectrum). The two-dimensional spectrum shows four distinct groups of peaks (the $\alpha\alpha$, $\alpha\beta$, $\beta\alpha$, and $\beta\beta$ group, see Fig. 1) which are due to the real coincidences of the hypersatellite and satellite K x-ray cascades and to the accidental coincidences of the diagram K x rays. In the original method of analysis[7] each of the four groups of peaks was analyzed separately. The new nonlinear least-squares routine allowed a simultaneous analysis of the section of the E_1-E_2 spectrum which included all four groups of hypersatellite-satellite peaks.

The two-dimensional function which was fitted to the E_1-E_2 spectrum was represented by 48 peaks, 8 ridges (bands), and a constant (the background). The peaks were represented by two-dimensional Gaussian functions of a variable width in either dimension and integrated over the channel limits. The numbers of counts in all symmetrical peaks and ridges (obtained by the exchange $E_1 \leftrightarrows E_2$) were assumed equal. This symmetry of response of the system with respect to the exchange of the two detector branches was checked carefully and proven to be very good. Accidental coincidences of the $K\alpha_2$, $K\alpha_1$, $K\beta_1$, and $K\beta_2$ (diagram) x rays were represented by 16 peaks (the dashed circles in Fig. 1). Only one variable parameter represented the numbers of counts in all 16 peaks, the number of counts in the $K\alpha_1$-$K\alpha_1$ peak. The numbers of counts in the remaining 15 peaks were assumed to follow from the known intensity ratios of the diagram lines,[8] taking into account the variation of the detector efficiency with energy.

Peaks due to the hypersatellite-satellite cascades were represented by 16 + 16 peaks (the solid circles in Fig. 1). Twelve variable parameters were used to represent the numbers of counts in the 16 pairs of peaks.

(i) One variable parameter was the number of counts

in the peaks due to the $K\alpha_1^h$-$K\alpha_1 L_3^{-1}$ cascade, $n(a_1)=n(a_2)$.

(ii) Three variable parameters were the intensity ratios of the hypersatellite transitions

$$I(K\alpha_2^h)/I(K\alpha_1^h)=[n(e)+n(f)+n(g)+n(h)]/n(K\alpha_1^h) ,$$
$$I(K\beta_1^h)/I(K\alpha_1^h)=[n(i)+n(j)+n(k)+n(1)]/n(K\alpha_1^h) ,$$
$$I(K\beta_2^h)/I(K\alpha_1^h)=[n(m)+n(n)+n(o)+n(p)]/n(K\alpha_1^h) ,$$

where $n(K\alpha_1^h)=n(a)+n(b)+n(c)+n(d)$, and $n(z)$ is the number of counts in the peak z, with $z=a_1,b_1,c_1,\ldots$, or $z=a_2,b_2,c_2,\ldots$.

(iii) Three variable parameters were the intensity ratios of the satellite transitions in atoms with an L_3-subshell spectator vacancy

$$I(K\alpha_2 L_3^{-1})/I(K\alpha_1 L_3^{-1})=n(b)/n(a) ,$$
$$I(K\beta_1 L_3^{-1})/I(K\alpha_1 L_3^{-1})=n(c)/n(a) ,$$
$$I(K\beta_2 L_3^{-1})/I(K\alpha_1 L_3^{-1})=n(d)/n(a) .$$

(iv) Three variable parameters were the intensity ratios of the satellite transitions in atoms with an L_2-subshell spectator vacancy

$$I(K\alpha_2 L_2^{-1})/I(K\alpha_1 L_2^{-1})=n(f)/n(e) ,$$
$$I(K\beta_1 L_2^{-1})/I(K\alpha_1 L_2^{-1})=n(g)/n(e) ,$$
$$I(K\beta_2 L_2^{-1})/I(K\alpha_1 L_2^{-1})=n(h)/n(e) .$$

(v) Two variable parameters were the following intensity ratios of the satellite transitions in atoms with an M- or N-shell spectator vacancy (these spectator vacancies were assumed to have the same effect on the intensity ratios):

$$I(K\beta_1 M^{-1})/I(K\alpha_1 M^{-1})=I(K\beta_1 N^{-1})/I(K\alpha_1 N^{-1})$$
$$=n(k)/n(i)=n(o)/n(m) ,$$
$$I(K\beta_2 M^{-1})/I(K\alpha_1 M^{-1})=I(K\beta_2 N^{-1})/I(K\alpha_1 N^{-1})$$
$$=n(l)/n(i)=n(p)/n(m) ,$$

while it was assumed $I(K\alpha_2 M^{-1})/I(K\alpha_1 M^{-1})=I(K\alpha_2 N^{-1})/I(K\alpha_1 N^{-1})=0.539$, i.e., equal to the corresponding ratio of the diagram lines.

The numbers of counts in each of the 4 + 4 ridges, which are due to the coincident detection of bremsstrahlung radiation in K-electron capture in ^{131}Cs and of the K x rays of xenon, were represented by a two-dimensional function of a Gaussian profile in one dimension and of a $1s$-bremsstrahlung profile in the other dimension. For low-energy internal bremsstrahling in ^{131}Cs electron-

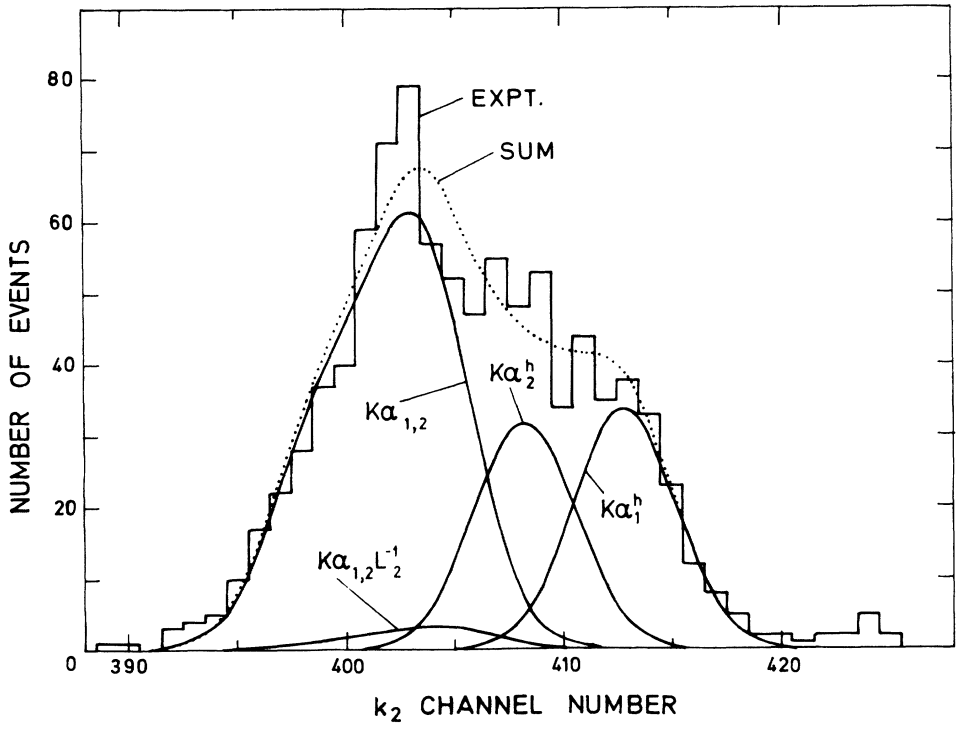

FIG. 2. Illustration of the result of fitting of a multicomponent surface to the E_1-E_2 spectrum. The histogram was obtained by projecting the two-dimensional spectrum onto the k_2 axis for $k_1=401-408$ ($E_1=29.41-29.96$ keV). Solid curves show the two-dimensional component functions obtained by the fitting routine and integrated over the same energy interval. Each curve is indicated by the corresponding K x-ray line. The dotted curve shows the sum of the solid curves. Its comparison to the histogram illustrates the goodness of the two-dimensional fit. Background was not subtracted from the data.

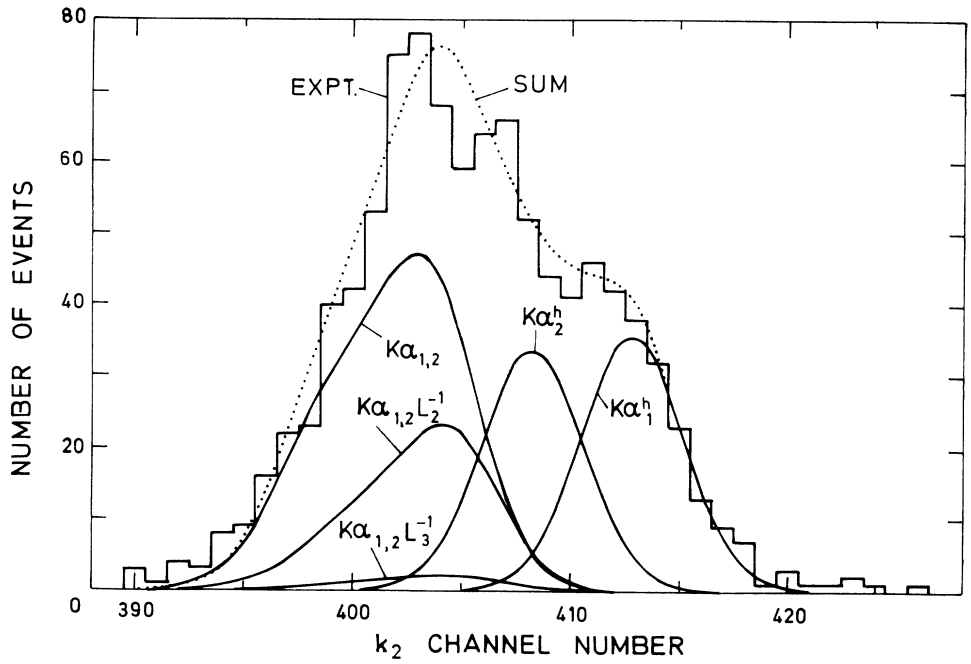

FIG. 3. Same as Fig. 2, but for $k_1 = 405-412$ ($E_1 = 29.68-30.14$ keV).

capture decay the relativistic correction factor is almost constant,[9] so a simple energy distribution, $E(E_{EC}-B_K-E)^2$, where $E_{EC}=355$ keV is the electron-capture transition energy and B_K the K-electron binding energy, was assumed. One variable parameter represented the numbers of counts in all eight ridges as it was assumed that the ratios of numbers of counts in the ridges are the same as for the corresponding diagram lines.

The energy scales (the k_1 and k_2 channel number to energy conversions) were defined via two variable reference points on each axis, the positions of the $K\alpha_1$ and $K\beta_1$ (diagram) lines (four variable parameters). The positions of the peaks due to the hypersatellite-satellite cascades were defined by the shifts from the corresponding diagram lines. Three variable parameters were used for the $K\alpha_{1,2}$, $K\beta_1$, and $K\beta_2$ hypersatellite shifts, and another three for the average values of the $K\alpha_{1,2}$, $K\beta_1$, and $K\beta_2$ satellite shifts due to a vacancy in the L_3 or L_2 subshell. The satellite shifts of the K x rays in atoms with a vacancy in the M or N shell (which are small and have a negligible effect on the results of the fit) have been fixed at values derived from an approximate calculation of energy shifts of electron levels due to the presence of a vacancy in atomic shells.[10]

Two variable parameters were used to define the widths of the peaks, one for the k_1 and the other for the k_2 dimension. The energy dependence of the widths was taken into account by assuming the Fano factor of 0.08 and an energy of 2.95 eV per electron-hole pair in germanium.

Equal weights and weights equal to the reciprocal numbers of counts (one for zero count[11]) were applied. The results of the two minimum χ^2 calculations are in good agreement for all variable parameters except for the numbers of counts in the $K\alpha_1$-$K\alpha_1$ and the $K\alpha_1^h$-$K\alpha_1 L_3^{-1}$ peaks. It is known[11] that the number of counts in a single

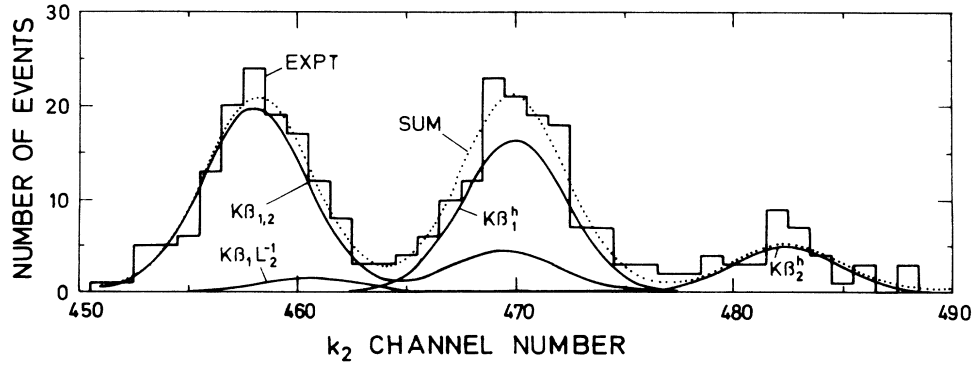

FIG. 4. Same as Fig. 2, but for $k_1 = 397-409$ ($E_1 = 29.13-30.03$ keV).

TABLE I. Hypersatellite and satellite energy shifts in xenon atoms (in eV).

Transition	Spectator vacancy	Results of	$\Delta(K\alpha)$	$\Delta(K\beta_1)$	$\Delta(K\beta_2)$
Hyper-		Theory[a]	639.4	814.9	
satellite	K	Theory[b]	639±10		
		This measurement	653±20	834±39	903±81
Satellite	L	Theory[b]	66±20		
		Theory[c]	79	178	
		Theory[d]	83	200	
		This measurement	80±15	169±34	261±81

[a]The weighted average value for the $K\alpha_2$ and $K\alpha_1$ lines (640.1 and 636.9 eV, respectively) of Chen, Crasemann, and Mark (Ref. 6) is quoted.
[b]Weighted averages of values calculated using the multiconfiguration Dirac-Fock code of Desclaux (Ref. 5), quoted in Ref. 3.
[c]Results of Hartree-Fock-Slater calculations reported in Burch, Wilets, and Meyerhof (Ref. 12).
[d]Burch, Wilets, and Meyerhof (Ref. 12) simple model.

peak calculated by a least-squares fit assuming Poisson statistics is low by the value of the χ^2. In the present analysis multiple two-dimensional peaks were encountered, so a simple addition of χ^2 was not possible. Therefore the results of the analysis with equal weights are reported, while the quoted errors were derived from the analysis with $1/n$ weights.

RESULTS AND DISCUSSION

The surface-fitting routine was devised in order to derive all results using only the E_1-E_2 spectrum. The fitting function, defined by the above described set of variable parameters (which included also the adjustment of the energy scales and of the widths of the peaks), is considered to represent very well the two-dimensional spectrum. All relevant parameters were varied simultaneously. Many checks were made (three are shown in Figs. 2–4). Hence the results of the fit are trusted to represent very well the measured spectrum. The errors were calculated by the inversion of the curvature matrix which was calculated using Poisson statistics, so they are also quite reliable.

Figures 2–4 illustrate the data and the fits for projections of three sections of the E_1-E_2 spectrum. As mentioned above, the background was very low and was not subtracted from the data shown in the figures. Figure 4 shows the relatively large shift of the $K\beta_2$ hypersatellite line. The results for the hypersatellite and satellite energy shifts are shown in Table I. The present results for the $K\alpha^h$ and $K\beta_1^h$ shift are in a very good agreement with the results of Chen *et al.*,[6] and of Desclaux (as quoted in Ref. 3). Energy shifts of the $K\alpha\, L^{-1}$ and $K\beta_1 L^{-1}$ satellite lines are also in a good agreement with the theoretical results of Desclaux (as quoted in ref. 3) and with the results of Burch, Wilets, and Meyerhof,[12] but the accuracy of the experimental results is not sufficient to discriminate between the theoretical results.

The results for the intensity ratios of the hypersatellite lines and of some satellite lines are shown in Table II. The results for the $I(K\alpha_2^h)/I(K\alpha_1^h)$, intensity ratio is larger than the theoretical result of Chen, Crasemann, and Mark[6] by about two standard deviations. Because of the disagreement, several checks of the fitting procedure were made, e.g., checks for local minima, different profiles of the bremsstrahlung spectrum, change of definition of variable parameters, such as introduction of intensity ratios $I(K\beta_1^h)/I(K\alpha_{1,2}^h)$ and $I(K\beta_2^h)/I(K_{1,2}^h)$ instead of the ratios $I(K\beta_1^h)/I(K\alpha_1^h)$ and $I(K\beta_2^h)/I(K\alpha_1^h)$, etc. However, the value of the ratio $I(K\alpha_2^h)/I(K\alpha_1^h)$

TABLE II. Intensity ratios of the hypersatellite and satellite transitions in xenon atoms.

Transition	Spectator vacancy	Results of	$I(K\alpha_2)/I(K\alpha_1)$	$I(K\beta_1)/I(K\alpha_1)$	$I(K\beta_2)/I(K\alpha_1)$
Hypersatellite	K	Theory[a]	0.658	0.297	
satellite		Previous measurement[b]	0.66±0.09		
		This measurement	0.94±0.18	0.36±0.06	0.09±0.04
Satellite	L_3	This measurement	0.44±0.10	0.24±0.05	0.09±0.05
Satellite	L_2	This measurement	0.44±0.09	0.26±0.05	0.05±0.04
Satellite	M or N	This measurement	assumed 0.539	0.33±0.15	0.07±0.09

[a]Calculated from the results for the transition probabilities of Chen, Crasemann, and Mark (Ref. 6).
[b]Isozumi, Briançon, and Walen (Ref. 3).

changed very little (by -0.02 to $+0.01$). A possible cause of the disagreement could be different angular distributions of $K\alpha_2^h - K \times L_2^{-1}$ and $K\alpha_1^h - K \times L_3^{-1}$ cascades. If this is the case a direct comparison of the ratio of the over-angle integrated theoretical intensities and of our result is not correct. An estimate was made on the number of events in which the absorption of a $K\alpha^h$ x ray in one detector and of a $K\alpha L^{-1}$ x ray in the other detector was accomplished by a simultaneous absorption of an L x ray in either one or the other detector. The effect on the $K\alpha_2^h$-to-$K\alpha_1^h$ intensity ratio is less than 1% (it tends to increase the ratio) and was neglected. The effect of deviation of the shape of peaks from the (in the fit assumed) Gaussian profile on the result of the $K\alpha_2^h$-to-$K\alpha_1^h$ intensity ratio was estimated at about 1% (it tends to decrease the ratio) and was neglected also. The difference between the present result and the result of Isozumi, Briançon, and Walen[3] amounts to 0.28 ± 0.20, i.e., it is not significant.

The results for the ratios of intensities of $K\alpha_2 L^{-1}$ and $K\alpha_1 L^{-1}$ satellite lines indicate values which are smaller than the value for the diagram lines.

From the numbers of counts in the peaks due to the hypersatellite-satellite cascades, the measured strengths of the ^{131}Cs sources (taking into account their decay), and from the calibrated efficiency of the detectors (scaling for energy variation according to the results of Ref. 13) the following probability of double-K-shell ionization per ^{131}Cs decay was determined:

$$P_{KK} = (1.48 \pm 0.35) \times 10^{-5} .$$

This result is in very good agreement with the previously determined value $(1.33 \pm 0.33) \times 10^{-5}$ of Isozumi, Briançon, and Walen.[3]

ACKNOWLEDGMENTS

This work was in part financially supported by the Scientific Council of the Republic of Croatia and the Federal Scientific Council of Yugoslavia, and in part by the National Science Foundation (Project No. PN-734).

[1] J. P. Briand, M. Tavernier, and J. P. Roset, Phys. Rev. Lett. **27**, 777 (1972).

[2] G. Schupp, H. J. Nagy, and A. Miles, Phys. Rev. C **36**, 2533 (1987), and references therein; C. W. E. van Eijk, J. P. Wagenaar, F. Bergsma, and W. Lourens, Phys. Rev. A **26**, 2749 (1982).

[3] Y. Isozumi, Ch. Briançon, and R. J. Walen, Phys. Rev. C **25**, 3070 (1982).

[4] B. Perny, J.-Cl. Dousse, M. Gasser, J. Kern, Ch. Rhême, P. Rymusa, and Z. Sujkowski, Phys. Rev. A **36**, 2120 (1987); S. I. Salem and A. Kumar, *ibid.* **28**, 2245 (1983).

[5] J. P. Desclaux, Comput. Phys. Commun. **9**, 31 (1975); J. P. Desclaux, Ch. Briançon, J. P. Thibaud, and R. J. Walen, Phys. Rev. Lett. **32**, 447 (1974); Ch. Briançon and J. P. Desclaux, Phys. Rev. A **13**, 2157 (1976).

[6] M. H. Chen, B. Crasemann, and H. Mark, Phys. Rev. A **25**, 391 (1982).

[7] V. Horvat and K. Ilakovac, Phys. Rev. A **31**, 1543 (1985).

[8] *Table of Isotopes,* 7th ed., edited by C. M. Lederer and V. S. Shirley (Wiley, New York, 1978).

[9] W. Bambynek, H. Behrens, M. H. Chen, B. Crasemann, M. L. Fitzpatrick, K. W. D. Ledingham, H. Genz, M. Mutterer, and R. L. Intemann, Rev. Mod. Phys. **49**, 77 (1977); R. L. Intemann, Phys. Rev. C **3**, 1 (1971).

[10] V. Horvat and K. Ilakovac (unpublished).

[11] P. R. Bevington, *Data Reduction and Error Analysis for the Physical Sciences* (McGraw-Hill, New York, 1969).

[12] D. Burch, L. Wilets, and W. E. Meyerhof, Phys. Rev. A **9**, 1007 (1974), and references therein.

[13] M. P. Fioratti and S. R. Piermatei, Nucl. Instrum. Methods **96**, 605 (1971).